2014 American Control Conference (ACC)
June 4-6, 2014. Portland, Oregon, USA

Adaptive Control of Aircraft Lateral Motion with an Unknown Transition to Nonmimimum-Phase Dynamics

Yousaf Rahman, Khaled Aljanaideh, Erol D. Sumer, and Dennis S. Bernstein

Abstract— **We apply retrospective cost adaptive control (RCAC) to a linearized aircraft dynamics with an unknown transition to nonminimum-phase (NMP) dynamics. In prior work, RCAC was used for command-following with unknown NMP zeros. In this work we extend those results to command following for cases where the dynamics transition from minimum-phase to NMP. We use system identification techniques to identify the NMP zero, and use this information in RCAC. We consider both full-state feedback and output feedback, and in both cases we follow step commands with transitioning dynamics. We first consider the case where RCAC is unaware of the change and NMP zero identification is unavailable to RCAC. We then assume that NMP zero information is available to RCAC from system identification.**

I. Introduction

The performance limitations of nonminimum-phase (NMP) zeros are inherent to fixed-gain feedback control [1], [2], [3]. Within the context of adaptive control, NMP zeros pose an additional challenge, namely, the tendency of the adaptive controller to cancel NMP zeros. This issue can be overcome with full-state feedback, but in many cases full state measurements are not available. Traditional output feedback model reference adaptive control is typically based on positive real conditions, which cannot be met for NMP systems [4], [5], [6]. In applications, however, such as aircraft flight control, robotics, and active vibration control [7], [8], [9], [10], NMP zeros arise due to sensor/actuator noncolocation. In these applications, NMP zeros are unavoidable, and developing techniques that can address this problem remains a research challenge.

To at least a limited extent, adaptive control laws have been developed to address the challenge of NMP zeros. For example, retrospective cost adaptive control (RCAC) has been shown to be effective for NMP systems with known NMP zeros [11]. For systems with unknown NMP zeros, a constrained optimization approach is used in [12] to prevent unstable pole-zero cancellation. However, it is clear that much remains to be done to address the effect of NMP zeros within adaptive control.

With this motivation in mind, the goal of the present paper is to consider the lateral dynamics of a flight vehicle under conditions of uncertainty that motivate the use of adaptive control. In particular, the lateral dynamics are assumed to transition from minimum phase to nonminimum phase. This scenario is reminiscent of the dynamics of a hypersonic vehicle in glide phase with unknown thermal effects [13], [14], [15]. The ultimate goal is to achieve reliable command following under the assumption that the transition occurs over an interval of time whose onset and duration are unknown and, in addition, the final NMP dynamics are also uncertain. As an intermediate step in addressing this problem, we consider the case where the details of the transition and the final NMP dynamics are known, provided by simultaneous identification. Retrospective Cost Model Refinement (RCMR) has been used for model refinement of a lateral dynamics model with erroneous modeling information in the presence of noisy and biased measurements [16]. Nevertheless, this objective is nontrivial since the adaptive control law must account for the transition from minimum-phase to NMP dynamics.

In the present paper we address this problem by applying RCAC in several ways, with the objective of ascertaining how this can problem can be best be addressed. After formulating the RCAC algorithm in Section 3, we proceed in Section 4 to consider the case of full-state feedback. In Section 5, we consider the output feedback case where only ϕ is available for feedback. Finally, in Section 6 we consider NMP zero identification.

Y. Rahman, K. Aljanaideh, E. D. Sumer, and D. S. Bernstein are with the Department of Aerospace Engineering, University of Michigan, Ann Arbor, MI, USA. {yousafrm, khaledfj, dogan, dsbaero}@umich.edu

II. Aircraft Model

We consider the lateral dynamics of an aircraft with a transition to NMP dynamics. We present the transition as follows. The dynamics are first expressed in terms of a nominal plant. Then, at an unknown time and in an unknown manner, the plant parameters transition from stable, minimum phase to stable, but NMP. We call the stable and minimum phase plant the *nominal* plant and the NMP plant the *off-nominal* plant.

The *nominal continuous-time* plant is given by

$$A_0 = \begin{bmatrix} -0.0771 & 0.269 & -0.9631 & 0.0397 \\ -25.60 & 0.0218 & 0.0995 & 0 \\ 0.6160 & 0.0376 & -0.2687 & 0 \\ 0 & 1 & -0.4202 & 0.0058 \end{bmatrix},$$

$$B_0 = \begin{bmatrix} -0.0002 \\ 2.519 \\ -0.0222 \\ 0 \end{bmatrix}, \tag{1}$$

and the *off-nominal continuous-time* plant is given by

$$A_1 = \begin{bmatrix} -0.0771 & 0.269 & -0.9631 & 0.0397 \\ -108.8 & 0.0218 & 0.0995 & 0 \\ 0.4107 & 0.0376 & -0.2687 & 0 \\ 0 & 1 & -0.4202 & 0.0058 \end{bmatrix},$$

$$B_1 = \begin{bmatrix} -0.0002 \\ 2.519 \\ -0.0665 \\ 0 \end{bmatrix}, \tag{2}$$

where $x = \begin{bmatrix}\beta & P & R & \phi\end{bmatrix}^{\mathrm{T}}$, that is, sideslip angle, roll rate, yaw rate, and roll angle.

Note that there are two parameter changes in A and one parameter change in B, and both plants are open-loop stable. Step commands are specified for the roll angle ϕ. Therefore, we consider two approaches, namely,

1) Full-State Feedback with dummy commands for β, P, and R; and
2) Output feedback with only ϕ available for feedback.

We discretize the nominal and off-nominal plants with $T_{\mathrm{s}} = 0.1$ sec. The discretized nominal and off-nominal plants are

$$A_{\mathrm{D0}} = \begin{bmatrix} 0.9553 & 0.0265 & -0.0934 & 0.0039 \\ -2.5210 & 0.9680 & 0.1310 & -0.0050 \\ 0.0551 & 0.0045 & 0.9708 & 0.0001 \\ -0.1282 & 0.0989 & -0.0369 & 1.0004 \end{bmatrix},$$

$$B_{\mathrm{D0}} = \begin{bmatrix} 0.0034 \\ 0.2492 \\ -0.0017 \\ 0.0126 \end{bmatrix}, \tag{3}$$

$$A_{\mathrm{D1}} = \begin{bmatrix} 0.9482 & 0.0255 & -0.0900 & 0.0038 \\ -10.3212 & 0.9595 & 0.5152 & -0.0210 \\ 0.0186 & 0.0041 & 0.9723 & 0.0001 \\ -0.5304 & 0.0953 & -0.0239 & 0.9999 \end{bmatrix},$$

$$B_{\mathrm{D1}} = \begin{bmatrix} 0.0036 \\ 0.2390 \\ -0.0061 \\ 0.0124 \end{bmatrix}. \tag{4}$$

All examples below use these discretized plant dynamics. Unless stated otherwise, we assume that the plant transition occurs at $t = 250$ sec and that it takes 10 sec to transition from the nominal plant to the off-nominal plant. We assume that all parameters vary simultaneously with a linear transition.

III. RCAC FORMULATION

Consider the MIMO discrete-time main system

$$x(k+1) = Ax(k) + Bu(k) + D_1 w(k), \tag{5}$$
$$y(k) = Cx + D_2 w(k), \tag{6}$$
$$z(k) = E_1 x(k) + E_0 w(k), \tag{7}$$

where $k \geq 0$, $x(k) \in \mathbb{R}^n$, $z(k) \in \mathbb{R}^{l_z}$ is the measured performance, $y(k) \in \mathbb{R}^{l_y}$ contains additional measurements that are available for control, $u(k) \in \mathbb{R}^{l_u}$ is the input signal, and $w(k) \in \mathbb{R}^{l_w}$ is the exogenous signal. The control-to-performance plant is defined by the transfer matrix

$$G_{zu} \triangleq E_1(zI - A)^{-1}B. \tag{8}$$

Furthermore, for each positive integer i, the i^{th} Markov parameter of G_{zu} is defined by

$$H_i \triangleq E_1 A^{i-1} B. \tag{9}$$

The goal is to develop an adaptive output feedback controller that minimizes the performance variable z in the presence of the exogenous signal w with limited modeling information about (5)-(7). The components of the signal w can represent either command signals to be followed, external disturbances to be rejected, or both, depending on the configurations of D_1 and E_0. We consider the following formulation of RCAC given in [17], [18], [19].

A. Control Law

We use the strictly proper time series control law

$$u(k) = \theta^{\mathrm{T}}(k)\phi(k-1), \tag{10}$$

where

$$\theta(k) = [N_1^{\mathrm{T}}(k) \ldots N_{n_c}^{\mathrm{T}}(k)\ M_1^{\mathrm{T}}(k) \ldots M_{n_c}^{\mathrm{T}}(k)]^{\mathrm{T}}, \tag{11}$$

$$\phi = [y^{\mathrm{T}}(k-1) \ldots y^{\mathrm{T}}(k-n_c)\ u^{\mathrm{T}}(k-1) \ldots u^{\mathrm{T}}(k-n_c)]^{\mathrm{T}}, \tag{12}$$

where, for all $1 \leq i \leq n_c$, $N_i(k) \in \mathbb{R}^{l_y \times l_u}$ and $M_i(k) \in \mathbb{R}^{l_u \times l_u}$. The control law 10 can be reformulated as

$$u(k) = \Phi(k-1)\Theta(k), \tag{13}$$

where

$$\Phi(k-1) = I_{lu} \otimes \phi^{\mathrm{T}}(k-1) \in \mathbb{R}^{l_u \times l_u n_c (l_u + l_y)}, \tag{14}$$
$$\Theta(k) = \mathrm{vec}(\theta(k)) \in \mathbb{R}^{l_u n_c (l_u + l_y)}, \tag{15}$$

"$\otimes$" denotes the Kronecker product, and "vec" is the column-stacking operator.

B. Retrospective Performance

For a positive integer n_{f}, we define

$$G_{\mathrm{f}}(\mathrm{q}) \triangleq D_{\mathrm{f}}^{-1}(\mathrm{q})\mathrm{N}_{\mathrm{f}}(\mathrm{q}), \tag{16}$$

where q is the forward shift operator, $n_{\mathrm{f}} \geq 1$ is the order of G_{f} and

$$N_{\mathrm{f}}(\mathrm{q}) \triangleq K_1 \mathrm{q}^{n_{\mathrm{f}}-1} + K_2 \mathrm{q}^{n_{\mathrm{f}}-2} + \cdots + K_{n_{\mathrm{f}}}, \tag{17}$$
$$D_{\mathrm{f}}(\mathrm{q}) \triangleq I_{l_z} \mathrm{q}^{n_{\mathrm{f}}} + A_1 \mathrm{q}^{n_{\mathrm{f}}-1} + A_2 \mathrm{q}^{n_{\mathrm{f}}-2} + \cdots + A_{n_{\mathrm{f}}}. \tag{18}$$

Furthermore, $K_i \in \mathbb{R}^{l_z \times l_u}$ for $1 \leq i \leq r$, $A_j \in \mathbb{R}^{l_z \times l_z}$ for $1 \leq j \leq r$, and each polynomial $D_{\mathrm{f}}(\mathrm{q})$ is asymptotically stable. The choice of G_{f} can be made based on Markov parameters, or the location of the nonminimum-phase zero. Next, for $k \geq 1$,we define the *retrospective performance variable*

$$\hat{z}(\hat{\Theta}(k), k) \triangleq z(k) + \Phi_{\mathrm{f}}(k-1)\hat{\Theta}(k) - u_{\mathrm{f}}(k), \tag{19}$$

where

$$\Phi_{\rm f}(k-1) \overset{\triangle}{=} G_{\rm f}({\rm q})\Phi_(k-1), \tag{20}$$

$$u_{\rm f} \overset{\triangle}{=} G_{\rm f}({\rm q})u(k), \tag{21}$$

and $\hat{\Theta}(k)$ is determined by the optimization below.

In this paper, $G_{\rm f}$ is chosen to be a finite-impulse-response (FIR) filter, that is, $A_j = 0$, for $1 \leq j \leq n_{\rm f}$.

C. Cumulative Cost and RCAC Update Law

For $k > 0$, we define the cumulative cost function

$$J(\hat{\Theta}(k), k) \overset{\triangle}{=} \sum_{i=1}^{k} \lambda^{k-i} \hat{z}^{\rm T}(\hat{\Theta}(k), i)\hat{z}(\hat{\Theta}(k), i) + \sum_{i=1}^{k} \lambda^{k-i}\eta(i)\hat{\Theta}^{\rm T}(k)\Phi_{\rm f}^{\rm T}(i-1)\Phi_{\rm f}(i-1)\hat{\Theta}(k) + \lambda^k(\hat{\Theta}(k)-\Theta_0)^{\rm T}P_0^{-1}(\hat{\Theta}(k)-\Theta_0), \tag{22}$$

where $\lambda \in \big(0, 1\big]$, $P_0 \in \mathbb{R}^{l_u n_c(l_u+l_y)\times l_u n_c(l_u+l_y)}$ is positive definite, $\eta(k) \overset{\triangle}{=} \eta_0 z^{\rm T}(k)z(k)$, and $\Theta_0 \in \mathbb{R}^{l_u n_c(l_u+l_y)}$. The following result follows from RLS theory [20].

Proposition 2.1: Let $P(0) = P_0$ and $\Theta(0) = \Theta_0$. Then, for all $k \geq 1$, the cumulative cost function (22) has a unique global minimizer $\Theta(k)$. Furthermore, $\Theta(k)$ is given by

$$\Theta(k) = \big[I - K(k)\Phi_{\rm f}(k-1)\big]\Theta(k-1) - P(k)\Phi_{\rm f}^{\rm T}(k-1)\big[z(k) - u_{\rm f}(k)\big], \tag{23}$$

where $P(k)$ satisfies

$$P(k) = \frac{1}{\lambda}\big[P(k-1) - K(k)\Phi_{\rm f}(k-1)P(k-1)\big], \tag{24}$$

and

$$K(k) = P(k-1)\Phi_{\rm f}(k-1)\Lambda(k)^{-1}, \tag{25}$$

$$\Lambda(k) = \frac{\lambda}{1+\eta(k)}I_{l_z} + \Phi_{\rm f}(k-1)P(k-1)\Phi_{\rm f}^{\rm T}(k-1). \tag{26}$$

D. NMP-Zero-Based Construction of $G_{\rm f}$

We construct the filter $G_{\rm f}$ such that the coefficients $K_1, \ldots K_{n_{\rm f}}$ are equivalent to $H_2 \times {\rm poly}({\rm NMP}_{\rm OSZ})$ for the full-state feedback case and $H_1 \times {\rm poly}({\rm NMP})$ for the output feedback case. For the full-state feedback case ${\rm poly}({\rm NMP}_{\rm OSZ})$ is a polynomial whose roots are equal to the NMP output subspace zeros. In the case where there are no NMP output subspace zeros, ${\rm poly}({\rm NMP}_{\rm OSZ}) = 1$. We explain output subspace zeros in Section 4. Similarly, for the output feedback case, ${\rm poly}({\rm NMP})$ is a polynomial whose roots are the NMP zeros. If there are no NMP zeros, then ${\rm poly}({\rm NMP}) = 1$.

IV. Full-State Feedback

We now apply a full-state feedback control law where we command all four states. The advantage of using full-state feedback is the lack of nonminimum-phase zeros in the transfer function G_{zu}. However, as shown below, output subspace zeros arise due to the nonsquare nature of the dynamics [21], and the plant may exhibit NMP behavior. The drawback of using full-state feedback is the need to provide commands for the three additional states, which is not straightforward in the presence of uncertain dynamics. To overcome this problem, we specify dummy commands for the states x_1, x_2, and x_3 given by

$$x_{1c}(k) = x_1(k-1), \tag{27}$$

$$x_{2c}(k) = x_2(k-1), \tag{28}$$

$$x_{3c}(k) = x_3(k-1), \tag{29}$$

where $x_{ic}(k)$ denotes the command of state x_i at step k.

A. Output-Subspace Zeros

A plant is nonsquare if $l_u \neq l_y$. In the case of the aircraft when using full state feedback, the plant is nonsquare. Since in this case, $l_y > l_u$, the plant is "tall". As shown in [21], RCAR implicitly squares the plant. We thus consider the notion of output-subspace zeros, which are the zeros from the control input to the scaled performance variable $H_i^{\rm T} z$, which drives the update of $\Theta(k)$, where H_i is the Markov parameter used by RCAC [21]. If G_{zu} is square or wide and has full rank, then $\mathcal{N}(H_i^{\rm T}) = \{0\}$. Therefore, $H_i^{\rm T} z = 0$ if and only if $z = 0$. In this case, it is reasonable to expect that the zeros from u to z and zeros from u to $H_i^{\rm T} z$ are identical. However, in the case where G_{zu} is tall, $\mathcal{N}(H_i^{\rm T})$ is a proper subspace of $\mathbb{R}^{l_z}$, and thus $H_i^{\rm T} z$ may be zero with nonzero z. In this case, the output-subspace zeros and the transmission zeros of G_{zu} may be distinct. In fact, in the full state feedback case, there are no transmission zeros but there may be output-subspace zeros. If the output-subspace zeros are NMP, then NMP behavior arises despite the use of full-state feedback.

B. Examples

Figure 1 shows command following when the NMP dynamics are unmodeled. Notice that in this case RCAC does not destabilize the closed-loop system. For this example, $n_c = 6$, $\eta_0 = 50$, $\lambda = 1$ and $P_0 = 1$. Figure 2 shows command following assuming NMP information is known throughout the flight. RCAC is able to follow the command despite having poor transient performance during and immediately after the transition to NMP dynamics. The adaptation is slower and a penalty is added to the control input at the expense of performance before the transition. Figure 3 shows the controller Θ. The controller converges before the transition, adapts and converges to different controller coefficients after the transition. For this example, $n_c = 40$, $\eta_0 = 3.5 \times 10^2$, $\lambda = 0.9997$ and $P_0 = 0.9$.

V. Output Feedback

We now consider output feedback, where measurements of only ϕ are available for feedback. We follow step commands for ϕ. In all cases, we assume that the plant transition occurs at $t = 250$ sec and that it takes 10 sec to transition from the nominal case to the off-nominal plant. We assume that

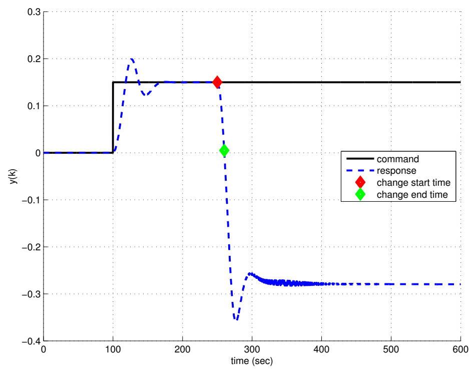

Fig. 1. Command following with unmodeled NMP dynamics. RCAC is able to follow the command until the transition to NMP behavior. After the transition, RCAC does not cause instability, but there is a large steady state error.

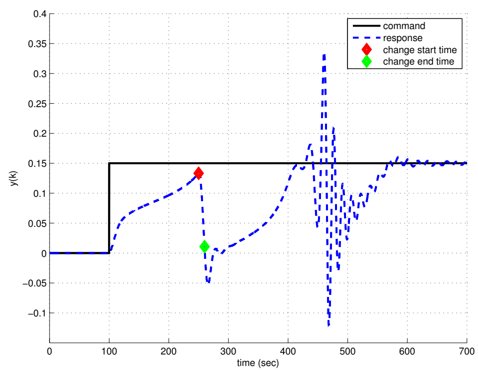

Fig. 2. Command following with NMP information. RCAC is able to follow the command throughout, despite poor transients and slow response before transition to NMP dynamics.

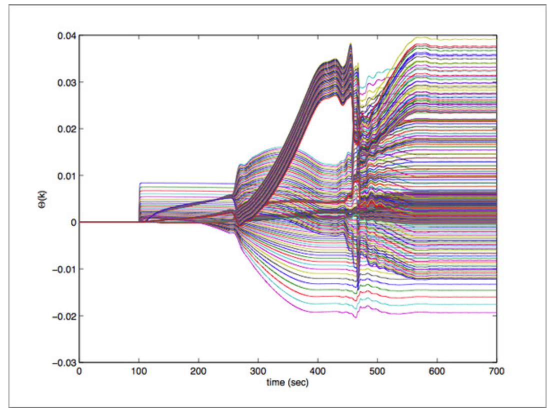

Fig. 3. Command following with NMP zero information. The controller coefficients converge before the transition, adapt and converge to different controller coefficients after the transition.

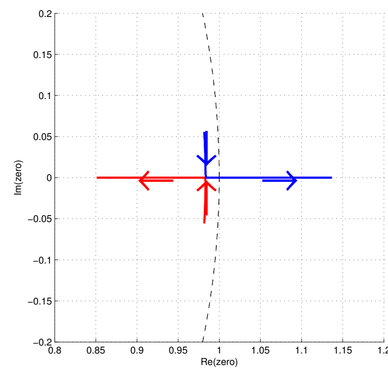

Fig. 4. Zero Locations. The two complex conjugate zeros become real and diverge along the real line. The transition to NMP dynamics occurs as the real zero crosses the unit circle.

all parameters vary simultaneously with a linear transition. The nominal plant has one real zero at -0.9959 and two complex zeros at $0.9818 \pm 0.0556j$. Figure 4 shows the transition of the two complex zeros as the system transitions from minimum phase to NMP. The two complex conjugate zeros become real and diverge along the real line. At the end of the transition, the plant has two NMP zeros at -1.0027 and 1.1369. Figure 5 shows the magnitude of the zeros as a function of time.

Figure 6 shows step command following with unmodeled NMP dynamics. Notice that in this case RCAC does not destabilize the closed-loop system. For this example, $n_c = 2$ and $\eta_0 = 50$. Figure 7 shows step command following in the case where NMP information is provided by system identification. After a transient, RCAC follows the command despite the transition to NMP dynamics. Figure 8 shows the controller Θ. The controller converges before the transition, and adapts and converges to different controller coefficients after the transition. The identified zeros are shown in Figure 9. For this example, $n_c = 15$ and $\eta_0 = 0$. In all cases, $\lambda = 1$, $P_0 = 0.5$. Note that the transition to NMP dynamics takes place over 1 sec, instead of 10 sec. RCAC performs better when using only output feedback, because the zeros of G_{zu} better describe the system than the output subspace zeros.

VI. NMP Zero Identification

To perform the identification process we use the μ-Markov model. For all $k \geq 0$, $\mu \geq 1$, and each model order $n_{\rm mod} \geq n$, the input $u(k)$ and the output $y(k)$ satisfy the μ-Markov model

$$y(k) = \sum_{j=0}^{\mu-1} H_j u(k-j) + \sum_{j=\mu}^{n_{\rm mod}+\mu-1} b_j u(k-j) - \sum_{j=\mu}^{n_{\rm mod}+\mu-1} a_j y(k-j), \qquad (30)$$

where $H_0, \ldots, H_{\mu-1}$ are Markov parameters of the system, that is, if the outputs $y(k-j)$ for all $j \in \{\mu, \ldots, n_{\rm mod}+\mu-1\}$ are zero and the input is the impulse $u(0) = 1, u(k) = 0$ for all $k > 0$, then the first μ outputs of (30) are the Markov parameters $H_1, \ldots, H_\mu$ of the system. Models of the form (30) are of interest because consistent estimation of $H_1, \ldots, H_\mu$ is possible in the presence of arbitrary output noise using standard least squares [22], [23] when the input u is white.

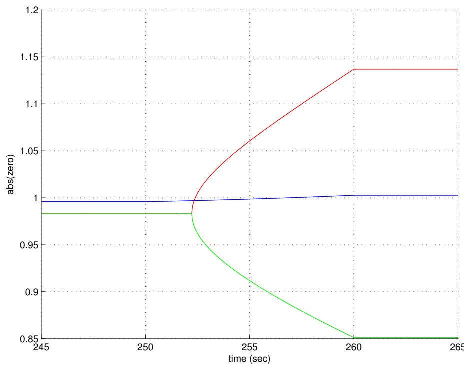

Fig. 5. Zero Magnitudes. The system becomes NMP at approximately $t = 252$ sec. The zero transitions to 1.1369 in 10 sec.

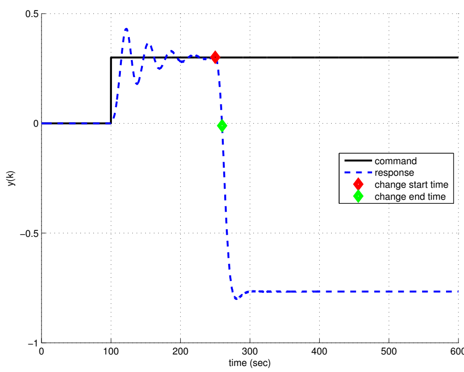

Fig. 6. Command following with unmodeled NMP dynamics. RCAC is able to follow the command until the transition to NMP behavior. After the transition, RCAC does not cause instability, but there is a large steady state error.

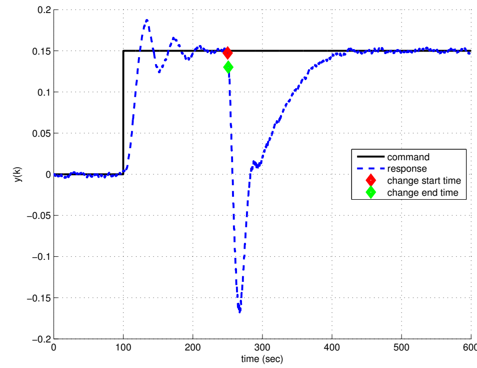

Fig. 7. Command flowing with NMP information provided by system identification. RCAC is able to follow the command throughout, and yields better performance than the full-state feedback case, with better minimum phase performance and quicker adaptation to NMP dynamics.

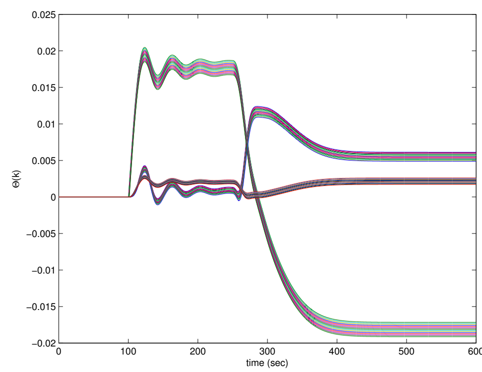

Fig. 8. Command following with NMP zero information. The controller coefficients converge before the transition, adapt and converge to different controller coefficients after the transition.

The μ-Markov model (30) can be expressed as

$$y(k) = \theta_\mu \phi_\mu(k) + \theta_u \phi_u(k) - \theta_y \phi_y(k), \tag{31}$$

where

$$\begin{aligned}
\theta_\mu &\triangleq \left[\begin{array}{ccc} H_0 & \cdots & H_{\mu-1} \end{array}\right], \\
\theta_u &\triangleq \left[\begin{array}{ccc} b_\mu & \cdots & b_{n_{\rm mod}+\mu-1} \end{array}\right], \\
\theta_y &\triangleq \left[\begin{array}{ccc} a_\mu & \cdots & a_{n_{\rm mod}+\mu-1} \end{array}\right], \\
\phi_\mu(k) &\triangleq \left[\begin{array}{ccc} u(k) & \cdots & u(k-\mu+1) \end{array}\right]^{\rm T}, \\
\phi_u(k) &\triangleq \left[\begin{array}{ccc} u(k-\mu) & \cdots & u(k-n_{\rm mod}-\mu+1) \end{array}\right]^{\rm T}, \\
\phi_y(k) &\triangleq \left[\begin{array}{ccc} y(k-\mu) & \cdots & y(k-n_{\rm mod}-\mu+1) \end{array}\right]^{\rm T}.
\end{aligned}$$

Least squares estimates $\hat{\theta}_{\mu,\ell}$, $\hat{\theta}_{u,\ell}$, $\hat{\theta}_{y,\ell}$ of θ_μ, θ_u, θ_y are given by

$$\left[\begin{array}{ccc} \hat{\theta}_{\mu,\ell} & \hat{\theta}_{u,\ell} & \hat{\theta}_{y,\ell} \end{array}\right] = \underset{[\,\bar{\theta}_\mu\ \bar{\theta}_u\ \bar{\theta}_y\,]}{\operatorname{argmin}} \left\| \Psi_{y,\ell} - \bar{\theta}_\mu \Phi_{\mu,\ell} - \bar{\theta}_u \Phi_{u,\ell} + \bar{\theta}_y \Phi_{y,\ell} \right\|_{\rm F}, \tag{32}$$

where $\bar{\theta}_\mu, \bar{\theta}_u, \bar{\theta}_y$ are variables of appropriate size, $||\,.\,||_{\rm F}$ denotes the Frobenius norm,

$$\begin{aligned}
\Psi_{y,\ell} &\triangleq \left[\begin{array}{ccc} y(n_{\rm mod}+\mu-1) & \cdots & y(\ell) \end{array}\right], \\
\Phi_{\mu,\ell} &\triangleq \left[\begin{array}{ccc} \phi_\mu(n_{\rm mod}+\mu-1) & \cdots & \phi_\mu(\ell) \end{array}\right], \\
\Phi_{u,\ell} &\triangleq \left[\begin{array}{ccc} \phi_u(n_{\rm mod}+\mu-1) & \cdots & \phi_u(\ell) \end{array}\right], \\
\Phi_{y,\ell} &\triangleq \left[\begin{array}{ccc} \phi_y(n_{\rm mod}+\mu-1) & \cdots & \phi_y(\ell) \end{array}\right],
\end{aligned}$$

and ℓ is the number of samples. Since we have a time-varying system, in order to track the change in the parameters with time we use a window of width of 70 data points moving 70 steps at a time to obtain the estimated Markov parameters. Once we obtain the estimated Markov parameters for a specific window we apply the eigensystem realization algorithm (ERA) [24] to reconstruct the system from its Markov parameters. ERA provides a state space realization, from which we construct a transfer function and find the zeros of the system. Figure 9 shows a plot of the modulus of all zeros of the system versus time. Note that before $t = 250$ sec the lateral dynamics have three minimum phase zeros while after $t = 265$ sec the lateral dynamics have

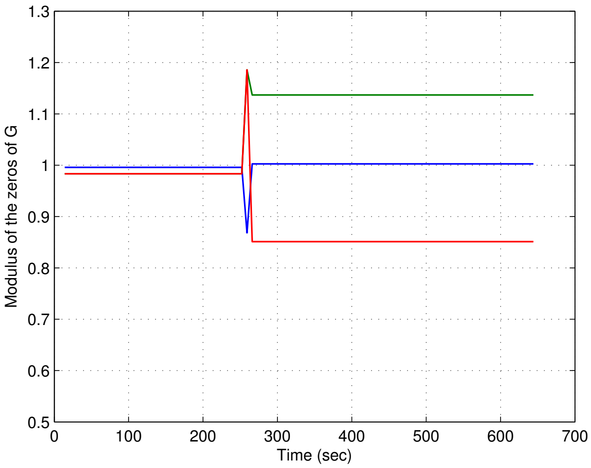

Fig. 9. Modulus of the zeros of the identified system. A window of width of 7 seconds and moving 7 seconds at a time is used to perform the identification process. Note that before $t = 250$ sec the lateral dynamics have three minimum phase zeros while after approximately $t = 265$ sec the lateral dynamics have two NMP zeros. Note the abrupt change in the modulus of the identified zeros between $t = 250$ sec and $t = 265$ sec as the transition data enter the identification process.

two NMP zeros.

VII. Conclusions

We used adaptive control together with system identification to control aircraft lateral motion with an unknown transition to NMP dynamics. We used retrospective cost adaptive control, which requires limited plant knowledge. We considered both the full-state-feedback case with output-subspace zeros and the output feedback case with NMP zeros. Even in the case where NMP zeros exist and are unmodeled, RCAC did not cause instability. A μ-Markov model along with standard least squares was used to identify the Markov parameters of the system given input-output data obtained using a moving window of a specific size. Then, the ERA was used to obtain a realization of the system from its Markov parameters, and the NMP zero information was be used by RCAC. Future work will consist of improving the response and identification during the transition from minimum phase to nonminimum phase behavior.

VIII. Acknowledgment

We wish to thank John Burken and Tim Cox for providing the lateral aircraft dynamics model and helpful discussions.

References

[1] J. B. Hoagg and D. S. Bernstein, "Nonminimum-Phase Zeros: Much to Do About Nothing," *IEEE Contr. Sys. Mag.*, vol. 27, no. June, pp. 45–57, 2007.

[2] B. R. Holt and M. Morari, "Design of resilient processing plants-vi. the effect of right-half-plane zeros on dynamic resilience," *Chem. Eng. Sci.*, vol. 40, pp. 59–74, 1985.

[3] D. P. Looze and J. S. Freudenberg, "Limitations of feedback properties imposed by open-loop right half plane poles," *IEEE Trans. Autom. Control*, vol. 36, pp. 736–739, 1991.

[4] H. K. Khalil, "Adaptive output feedback control of nonlinear systems represented by input-output models," *Automatic Control*, vol. 41, pp. 177–188, 1996.

[5] B. M. Mirkin and P. O. Gutman, "Decentralized output-feedback mrac of linear state delay systems," *Automatic Control*, vol. 48, pp. 1613–1619, 2003.

[6] M. Bodson and J. E. Groszkiewicz, "Multivariable adaptive algorithms for reconfigurable flight control," *Control Systems Technology*, vol. 5, pp. 217–229, 1997.

[7] J. Yan, J. B. Hoagg, R. E. Hindman, and D. S. Bernstein, "Longitudinal Aircraft Dynamics and the Instantaneous Acceleration Center of Rotation: The Case of the Vanishing Zeros," *IEEE Contr. Sys. Mag.*, vol. 30, pp. 68–92, 2011.

[8] E. H. Maslen, "Positive real zeros in flexible beams," *Shock and Vibration Digest*, vol. 2, pp. 429–435, 1995.

[9] D. K. Miu, *Mechatronics: Electromechanics and Contromechanics*. New York: Springer Verlag, 1993.

[10] A. V. Morozov, J. B. Hoagg, and D. S. Bernstein, "Retrospective adaptive control of a planar multilink arm with nonminimum-phase zeros," in *Proc. Conf. Dec. Contr.*, Atlanta, GA, December 2010, pp. 3706–3711.

[11] J. B. Hoagg and D. Bernstein, "Retrospective Cost Model Reference Adaptive Control for Nonminimum-Phase Systems," *AIAA J. Guid. Contr. Dyn.*, vol. 35, pp. 1767–1786, 2012.

[12] A. Morozov, A. M. D'Amato, J. B. Hoagg, and D. S. Bernstein, "Retrospective cost adaptive control for nonminimum-phase systems with uncertain nonminimum-phase zeros using convex optimization," in *Proc. Amer. Contr. Conf.*, San Francisco, CA, June 2011, pp. 1188–1193.

[13] M. A. Bolender and D. B. Doman, "Flight path angle dynamics of airbreathing hypersonic vehicles," in *Proc. AIAA Guid. Nav. Contr. Conf.*, Keystone, CO, August 2006, AIAA-2006-6692.

[14] B. Xu, D. Wang, F. Sun, and Z. Shi, "Direct neural control of hypersonic flight vehicles with prediction model in discrete time," *Neurocomputing*, vol. 115, pp. 39–48, 2013.

[15] Q. Wei and X. Huang, "Lateral stability analysis of hypersonic vehicle under pressure fluctuation by solving mathieu differential equation," *arXiv*, p. arXiv:1204.2490, 2012.

[16] Y. Rahman, J. Zhong, A. Morozov, and D. S. Bernstein, "On the accuracy of state estimators for constant and time-varying parameter estimation," in *Proc. AIAA Guid. Nav. Contr. Conf.*, Boston, MA, August 2013, AIAA-2012-5192.

[17] E. D. Sumer, A. M. D'Amato, A. M. Morozov, J. B. Hoagg, and D. S. Bernstein, "Robustness of retrospective cost adaptive control to markov-parameter uncertainty," in *Proc. Conf. Dec. Contr.*, Orlando, FL, December 2011, pp. 6085–6090.

[18] E. D. Sumer and D. S. Bernstein, "Adaptive control of flexible structures with uncertain dynamics and uncertain disturbance spectra," in *Proc. AIAA Guid. Nav. Contr. Conf.*, Minneapolis, MN, August 2012, AIAA-2012-4437-323.

[19] E. D. Sumer and D. S. Bernstein, "Retrospective cost adaptive control with error-dependent regularization for mimo systems with uncertain nonminimum-phase transmission zeros," in *Proc. AIAA Guid. Nav. Contr. Conf.*, Minneapolis, MN, August 2012, AIAA-2012-4670-123.

[20] K. J. Astrom and B. Wittenmark, *Adaptive Control*, 2nd ed. Addison-Wesley, 1995.

[21] E. D. Sumer and D. S. Bernstein, "On the role of subspace zeros in retrospective cost adaptive control of nonsquare plants," submitted.

[22] M. Kamrunnahar, B. Huang, and D. B. Fisher, "Estimation of Markov Parameters and Time-delay/Interactor Matrix," *Chemical Engineering Science*, vol. 55, pp. 3353ï¿½3363, 1999.

[23] M. S. Fledderjohn, M. S. Holzel, H. Palanthandalam-Madapusi, R. J. Fuentes, and D. S. Bernstein, "A Comparison of Least Squares Algorithms for Estimating Markov Parameters," in *Proc. Amer. Contr. Conf.*, Baltimore, MD, June 2010, pp. 3735–3740.

[24] J. N. Juang, *Applied System Identification*. Upper Saddle River, NJ: Prentice-Hall, 1993.